ID: 2016-ISFT-243

A Study on Design of Waveguide Reactance Element for Introductory Microwave Experiment

Yusuke Kusama[1], Osamu Hashimoto[2]

[1,2]*National Institute of Technology, Kagawa College, 551 Kouda, Takuma-cho, Mitoyo-shi, Kagawa, 769-1192 Japan*
[1]*kusama@cn.kagawa-nct.ac.jp*

Abstract: *The use of the triple combination of theory, simulation, and experiment is most commonly used to promote better understanding among students. As part of the RF engineers training education program, we have studied to develop an advanced experimental program in which students can experience succeeding trial and error procedures such as design, circuit fabrication, simulation, and measurement. As a result, we expect that it is possible to learn the basis of practicable microwave circuit design procedures in the College of Technology. In this paper, the design theory and production evaluation process are focused on the waveguide inductive and capacitive window.*

Keywords: *Microwave Circuit, Waveguide, Technical Education, School Education, CAD*

1. INTRODUCTION

Microwave products become something familiar to the public by widespread use of mobile communications, wireless LAN, GPS and automotive radar. From the perspective of the frequency allocation and reorganization policy presented by Ministry of Internal Affairs and Communications (MIC) in Japan, the higher frequency of the carrier is expected to be further accelerated for performing the effective use and efficient information transmission of high demand frequency band. Therefore, it is essential to cultivate a deep theoretical knowledge and practicable elemental technologies to cope with microwaves as a competent engineer. However, human resources with specialized knowledge and practicable technology of microwave circuit and antenna design, so-called "RF Design", is said to be in a chronic shortage [2]. To survive in the field of RF design technology in the future, it is necessary and urgent need for a large number of RF engineers with excellent sense and creativity at the early stage. It is necessary to experience a large number of the experimental facts in parallel with the theory behind supporting them using the help of the simulator to train the RF engineers who can exert the ingenious design perspective. Then both theoretical knowledge and practicable techniques are synergistically deepened [3].

Although it is fundamental to acquire theoretical knowledge by the lecture, microwave engineering consists of versatile subjects such as material, circuit, module, antenna, system, measurement, error analysis, theoretical mathematics, programming, and simulator. So it is like a jigsaw puzzle made of pieces over. To support a beginner, there is a need to repeat a systematic arrangement and maintenance of these puzzle pieces in accordance with the progress of the times and technology. While this is required a great deal of effort and cost, such as the flip teaching or remote teaching delivery using the web as part of the active learning, it is seemed that there is room for further improvement by the development of information and communication technology.

On the other hand, for the measurement and evaluation, creativity and good sense as an expert are gradually cultivated by repeated experience of trial and error cycle unique to the RF design, that is design ⇒ simulation ⇒ production ⇒ measurement evaluation ⇒ problem discovery thinking and solving ⇒ redesign. Generally, such a cycle was experienced only part of the technician in the company, it is the objective of the present study to introduce and expand the experimental program that can experience early in higher educational institutions, including the National College of Technology. Attempt for such microwave education what should be the reference have been many reports in foreign countries, such as the use of computer aided design (CAD), Computer aided engineering (CAE) package integrated video materials and simulator, theoretical calculation, design exercises, measurement training, and introduction of microwave education courses in each university [4 - 8]. In Japan, several efforts example of specialized education programs for graduate students or working people have been reported [9-11].

In such background, in the microwave experiment for 5[th] grade students of department of communication network engineering, NIT KC, in order to perform the derivation of the high frequency load impedance by using the waveguide standing-wave pattern measurement, an experimental program that combines measurement, theoretical calculation, and simulation are introduced [12]. Although in the previous experiment, the three different load conditions

(short, open, and load) that make up a commonly used calibration standard are examined, inductance or capacitance load which has important role in understanding the Smith chart have not been considered. So in order to newly introduce such reactance elements, we have reported on the evaluation results of the simplified samples fabricated as a preliminary test [13]. In this study, several new waveguide reactance elements are remanufactured as the experimental standards to eliminate the influence of manufacturing error and investigated. Good agreement is obtained compared with exact solution.

2. CALCULATION THEORY

2.1 EQUIVALENT CIRCUIT ANALYSIS

Most familiar waveguide L, C elements can be expressed by changing the length of the short ended waveguide with shunt connection and it is obtained apparently reactance shift. Another method is expressed by inserting the electric wall in the waveguide cross section. Although, the latter is somewhat cumbersome method compared to the former, it is an effective approach to miniaturization of the circuit. These are commonly referred to as inductive window or capacitive windows, relation between the electric wall size and the shunt equivalent circuit element values are obtained [14]. For example, it is possible to make a window of width d in the waveguide section by inserting the metal wall of width a-d shown in the upper part in Fig.1. Where a is a waveguide width, b is the waveguide height. The z-axis is the propagation direction. Since the magnetic field is generated in the xz plane to avoid the inserted metal wall, the magnetic field is generated around the metal wall. In this case the inductive reactance is obtained on the metal wall by the current flow in the y-axis direction. The normalized susceptance corresponding to the upper part of the inductive window L1 and L2 in Fig. 1 are shown in Equation (1) and (2). Here Y_0 is characteristic admittance of the waveguide, B is susceptance of inductive window, λg is the guided wavelength of the waveguide TE_{10} mode. The corresponding equation for structure L3 is omitted.

$$\frac{B}{Y_0} = -\frac{\lambda_g}{a}\left\{1+\operatorname{cosec}^2\left(\frac{\pi d}{2a}\right)\right\}\cot^2\left(\frac{\pi d}{2a}\right) \tag{1}$$

$$\frac{B}{Y_0} = -\frac{\lambda_g}{a}\cot^2\left(\frac{\pi d}{2a}\right) \tag{2}$$

Similarly, it is possible to make the window of the vertical width d in the waveguide section by inserting the metal wall of width b-d shown in the bottom in Figure 1. Thus interval of waveguide E-plane is narrowed by inserting a metal wall, the electric field is concentrated in the yz plane. In this case the capacitive reactance is obtained on the metal wall gap by the charge storage in the y-axis direction. The normalized susceptance corresponding to the lower part of the capacitive windows C1 and C2 in Figure 1 are shown in Equation (3) and (4). The corresponding equation for structure C3 is omitted.

$$\frac{B}{Y_0} = \frac{8b}{\lambda_g}\ln\left\{\operatorname{cosec}\left(\frac{\pi d}{2b}\right)\right\} \tag{3}$$

$$\frac{B}{Y_0} = \frac{4b}{\lambda_g}\ln\left\{\operatorname{cosec}\left(\frac{\pi d}{2b}\right)\right\} \tag{4}$$

As from the equation (1) to (4), it is very useful the value of the element is given as a function in advance because beginners can derive calculation value easily in Excel though derivation of these equations are even as advanced content. When measuring such a device under test (DUT) elements in waveguide systems, it is considered an equivalent circuit as shown in Figure 2. The normalized input impedance zin shown from Port1 is the parallel connection of B and Y0. It is given by

$$z_{\text{in}} = \frac{Z_{\text{in}}}{Z_0} = \frac{1}{y_{\text{in}}} = \frac{1}{1+jb} = \frac{1}{1+b^2} + j\frac{-b}{1+b^2} \tag{5}$$

Here, Y_0 is the characteristic admittance of waveguide TE_{10} mode, $b = B/Y_0$ is a normalized susceptance of the DUT. Therefore, reflection coefficient Γ from Port1 is given by

$$\Gamma = \frac{Z_{\text{in}} - Z_0}{Z_{\text{in}} + Z_0} = \frac{z_{\text{in}} - 1}{z_{\text{in}} + 1} = \frac{(\alpha + j\beta) - 1}{(\alpha + j\beta) + 1} \tag{6}$$

And the real part and imaginary part of the reflection coefficient is given by the following equations.

$$\operatorname{Re}[\Gamma] = \frac{\alpha^2 + \beta^2 - 1}{(\alpha+1)^2 + \beta^2} = \operatorname{Re}[S_{11}] \tag{7}$$

$$\operatorname{Im}[\Gamma] = \frac{2\beta}{(\alpha+1)^2 + \beta^2} = \operatorname{Im}[S_{11}] \tag{8}$$

Here, the α and β in equation (6) to (8) represents the real part and the imaginary part of the normalized impedance of equation (5), it is the respective next value.

$$\alpha = \frac{1}{1+b^2}, \quad \beta = \frac{-b}{1+b^2} \tag{9}$$

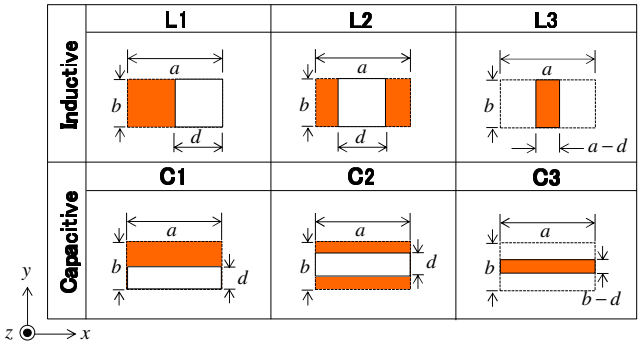

Fig. 1. Examples of inductive window and the capacitive window

a×b is the original waveguide cross section, d represents the window size. L1; C1 are the window structure of one side only, L2; C2 are center window structure, L3; C3 are the center post structure..

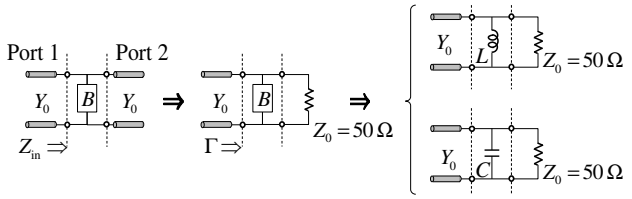

Fig. 2. Equivalent circuits for the DUT measurement.

2.2 MODE MATCHING METHOD

Equivalent circuit analysis of the previous section 2.1 is a simple expression that focuses on the TE_{10} dominant mode. So it is necessary to take into account the higher-order modes that occur in the vicinity of the window. To cope with these problems, an electromagnetic field simulator capable of full-wave analysis or the mode matching method to connect the mode series sum expressed in the form of eigenfunction expansion at the boundary surfaces are known [15-16]. Analysis of the inductive window is reduced to H-plane discontinuity problem, although the analysis of the capacitive window is reduced to E-plane discontinuity problems. It will be described here only the latter. Consider no discontinuity in the waveguide x direction as shown in Figure 3. When the driven mode can be assumed to TE_{m0}, the electric field component E_x does not occur structurally. Thus, it can be developed with TE_x (LSE_x mode) considering the five electromagnetic field components [17]. By using the following electric vector potential F

$$\mathbf{F}^{+} = \hat{x}F_x^{+} = \hat{x}F_{mn}\sin\left(\frac{m\pi}{a}x\right)\cos\left(\frac{n\pi}{b}y\right)e^{-jk_z z} \tag{10}$$

$$\mathbf{F}^{-} = \hat{x}F_x^{-} = \hat{x}B_{mn}\sin\left(\frac{m\pi}{a}x\right)\cos\left(\frac{n\pi}{b}y\right)e^{+jk_z z} \tag{11}$$

The electromagnetic field of the TE_x mode can be expressed by the following equation.

$$E_x = 0, \qquad H_x = -j\frac{1}{\omega\mu\sigma}\left(\frac{\partial^2}{\partial x^2} + \omega^2\mu\varepsilon\right)F_x \tag{12}$$

$$E_y = -\frac{1}{\varepsilon}\frac{\partial F_x}{\partial z}, \quad H_y = -j\frac{1}{\omega\mu\varepsilon}\frac{\partial^2 F_x}{\partial x\partial y} \tag{13}$$

$$E_z = \frac{1}{\varepsilon}\frac{\partial F_x}{\partial y}, \quad H_z = -j\frac{1}{\omega\mu\varepsilon}\frac{\partial^2 F_x}{\partial x\partial z} \tag{14}$$

For example, in order to apply the boundary condition at the discontinuity z=0, the n-th mode of the transverse electromagnetic field set of Ey, H_x are expressed by

$$E_y = G_n\sin(k_x x)\cos(k_y y)\left(F_n e^{-jk_z z} + B_n e^{+jk_z z}\right) \tag{15}$$

$$H_x = -G_n Y_n\sin(k_x x)\cos(k_y y)\left(F_n e^{-jk_z z} - B_n e^{+jk_z z}\right) \tag{16}$$

Here, fixed m=1 for the TE_{10} mode input. The wave number kz, cutoff wave number kc, and admittance Y_n is given by equation (17) to (19).

$$k_z = \begin{cases}\sqrt{k_0^{\,2} - k_c^{\,2}} & (k_0 > k_c)\\ -j\sqrt{k_c^{\,2} - k_0^{\,2}} & (k_0 < k_c)\end{cases} \tag{17}$$

$$k_c = \sqrt{k_x^{\,2} + k_y^{\,2}} = \sqrt{\left(\frac{\pi}{a}\right)^2 + \left(\frac{n\pi}{b}\right)^2} \tag{18}$$

$$Y_n = \frac{k_0^{\,2} - k_x^{\,2}}{\omega\mu k_z} \tag{19}$$

Also, G_n of the equation (20) is an normalized amplitude when transmitted power of the propagation mode in z-direction is 1W and also, transmitted power of the non-propagation mode is j1 W. Here, ε_n is a symbol shown in equation (21).

$$G_n = \begin{cases}\sqrt{\dfrac{\varepsilon_n}{ab}\dfrac{1}{Y_n}} & (k_0 > k_c)\\ \sqrt{\dfrac{\varepsilon_n}{ab}\dfrac{-j}{Y_n}} & (k_0 < k_c)\end{cases} \tag{20}$$

$$\varepsilon_n = \begin{cases}1 & (n = 0)\\ 2 & (n \geq 1)\end{cases} \tag{21}$$

Then, the boundary conditions of the following equation (22) (23) are applied at the z = 0 plane. Although the right-hand side bottom in equation (23) correspond to the wall current, it may remain unknown.

$$\sum_{n=0}^{N} G_n^{I}\cos(k_y^{I} y)\left(F_n^{I} + B_n^{I}\right) = \begin{cases}\sum_{q=0}^{Q} G_q^{II}\cos(k_y^{II} y)\left(F_q^{II} + B_q^{II}\right) & 0 \leq y \leq b_2\\ 0 & b_2 \leq y \leq b_1\end{cases} \tag{22}$$

$$\sum_{n=0}^{N} -G_n^{I} Y_n^{I}\cos(k_y^{I} y)\left(F_n^{I} - B_n^{I}\right) = \begin{cases}\sum_{q=0}^{Q} -G_q^{II} Y_q^{II}\cos(k_y^{II} y)\left(F_q^{II} - B_q^{II}\right) & 0 \leq y \leq b_2\\ ? & b_2 \leq y \leq b_1\end{cases} \tag{23}$$

Furthermore, in order to use the mode orthogonality, equation (22) is multiplied by $\cos(k_{1y}y)$ and integrated over the range from 0 to b_1 and also equation (23) is multiplied by $\cos(k_{2y}y)$ and integrated over the range from 0 to b_2 each. Finally, they are summarized in the simultaneous equations shown in equation (24) [18]. In this study, the highest order

mode number of both region I and II are determined N = Q = 100 on confirming the modal convergence. Here, L_E, L_H are expressed in the form of equation (25) and (26). Although, these calculations include integral, the integral calculation is avoidable by using the addition theorem [19]. In the case of the capacitive window, a structure obtained by mirror-reversed image of Figure 3 needs to be cascaded to the right through the thickness of the sample [20].

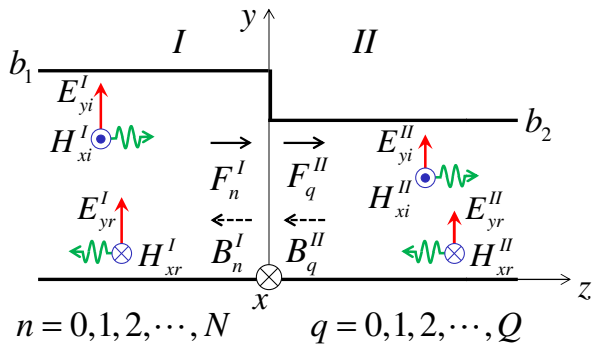

Fig. 3. Modal analysis model of E plane discontinuity for TE_x (LSE_x) mode.

$$\begin{cases} F_n^I + B_n^I = \sum_{q=0}^{Q} [L_E]_{n,q} \left[F_q^{II} + B_q^{II} \right] \\ \sum_{n=0}^{N} [L_H]_{q,n} \left[F_n^I - B_n^I \right] = F_q^{II} - B_q^{II} \end{cases} \quad (24)$$

$$[L_E]_{n,q} = \frac{\varepsilon_n G_q^{II}}{b_1 G_n^I} \int_0^{b_2} \cos(k_y^{II} y) \cos(k_y^I y) dy \quad (25)$$

$$[L_H]_{q,n} = \frac{\varepsilon_q G_n^I Y_n^I}{b_2 G_q^{II} Y_q^{II}} \int_0^{b_2} \cos(k_y^I y) \cos(k_y^{II} y) dy \quad (26)$$

F_{1n} and B_{1n} (n=0,1,2,…,N) are the normalized amplitude of n^{th} order incident wave and reflected wave in region I. F_{2q} and B_{2q} (q=0,1,2,…,Q) are the normalized amplitude of n^{th} order incident wave or reflected wave in region II.

2.3 MEASUREMENT SAMPLES

The sample shapes of the inductive window are shown in Figure 4 left. Inductive windows were manufactured two kinds. One is the case of inserting the step structure only in the one side of the waveguide H-plane and the other is a symmetrical step structure. The prepared window sizes are the following three types of 80%, 50% and 20% with respect to the original waveguide cross section. Also, the sample shapes of capacitive window are shown in Figure 4 right. Capacitive windows were manufactured also two kinds. One is the case of inserting the step structure only in the top side of the waveguide E-plane and the other is a symmetrical step structure. The prepared window sizes are the following three types of 80%, 50% and 20% with respect to the original waveguide cross section. The X-band standard waveguide WR-90 flange was used with Ag plated phosphor bronze. The thickness of the sample is sufficiently thin with respect to the wavelength, and was 0.5 mm so as to maintain the strength required for the measurement operation. It is also possible to own process using a commercially available copper plate as long as the thickness of this level.

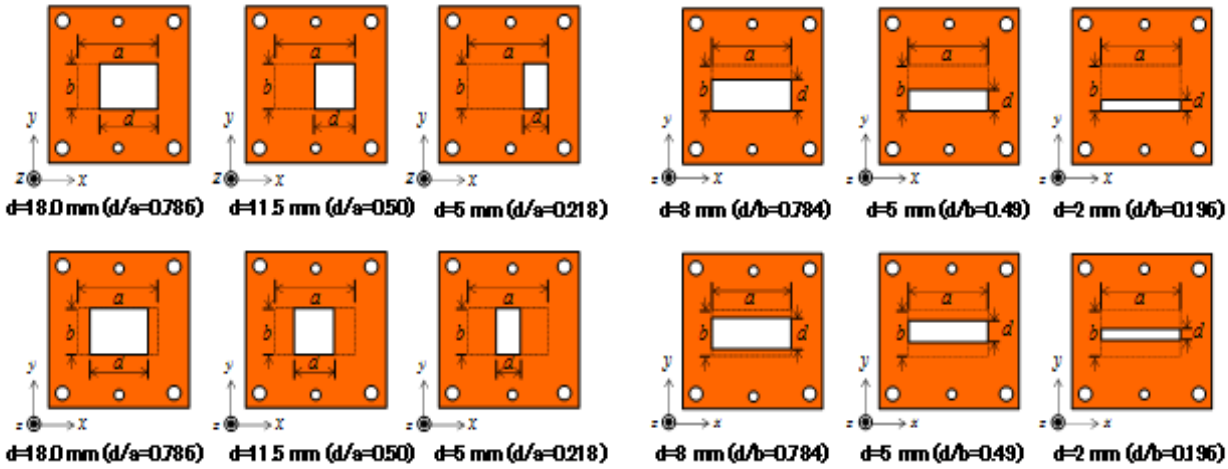

Fig. 4. Inductive window samples (left). From top left L1, L2, L3, and from the lower left L4, L5, L6. Capacitive window samples (right). From top left C1, C2, C3, and from the lower left C4, C5, C6. 0.5 mm thickness phosphor bronze with WR-90 standard waveguide flange is used.

3. MEASUREMENT SYSTEM

The measurement system is shown in Figure 5. The tip of WR-90 coaxial to waveguide adapter is set to the calibration plane. The reflection characteristics S_{11} were measured in the frequency range from 8.2 to 12.4 GHz inserting the measurement sample into the calibration plane. The vector network analyzer (VNA) Agilent E8362C is used using the following conditions, IF bandwidth 1 kHz, the number of measurement points is 401.

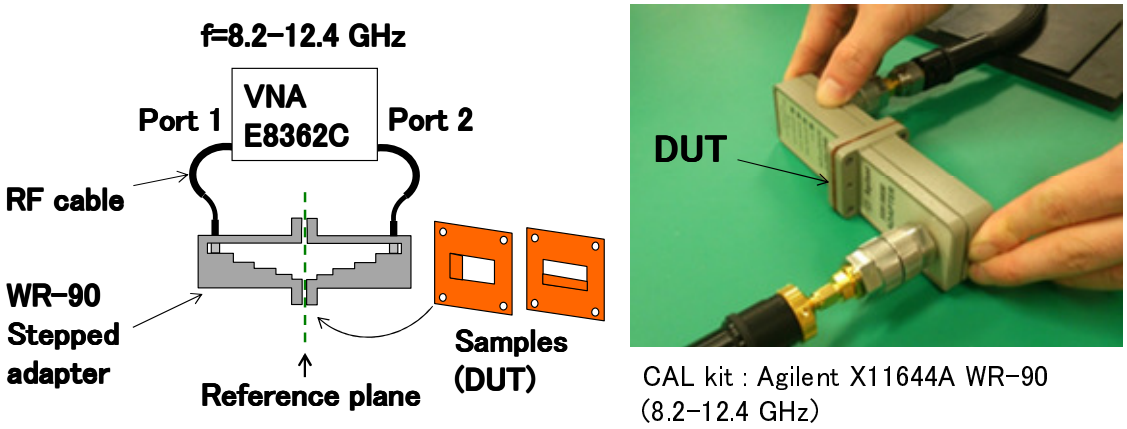

Fig. 5. Schematic view of the measurement system. The calibration plane is set to the center of the WR-90 stepped coaxial to waveguide adaptor. The vector network analyzer (VNA) of Agilent E8362C is used for frequency range from 8.2 to 12.4 GHz, IF bandwidth 1 kHz, the number of measurement points is 401.

4. RESULTS

Results of the inductive windows are shown in Figure 6. The vertical axis is the reflection coefficient [dB] and the horizontal axis is the frequency [GHz]. Three types of data indicate measured value (Meas.), equivalent circuit calculation (Circ.), and mode matching method (MM.). Focusing on L1 in Figure 6 top left, the cut-off frequency 6.5 GHz of the input TE_{10} and the cut-off frequency 13 GHz of the TE_{20} can be confirmed by the mode matching method. Measured value and mode-matching method is in good agreement, but the calculation error becomes larger near the cut-off frequency of the TE_{20} mode by the equivalent circuit calculation. This trend is same with L2 which has relatively large reflection. Note that L3 is almost total reflection, it is difficult to distinct the difference between three data. On the contrary, looking at L1 in Figure 6 left, it is not able to be confirmed TE_{20} cut-off frequency seen in Figure 6 right. This is because the higher order mode of even-number does not occur in a symmetrical structure. Although the mode matching method is in good agreement with the measured values in all case, the larger the error of the equivalent circuit calculation is if the reflection is small as in the case of L4. Moreover, in comparison to Figure 6 left and right, it can be seen that the reflection coefficient varies by the relationship between the electromagnetic field distribution of the input mode and the window structure even though the window size is same.

Similarly, Results of the capacitive window are shown in Figures 7. First, paying attention to the C1 in Figure 7 left, the mode matching method and the equivalent circuit calculation are in good agreement. However, there is a significant difference between both calculation data and the measured value compared with the case of the inductive window. In addition, in some cases in C2 and C3, the equivalent circuit calculation is close to the measured value than the exact mode matching method. It is considered that there is a reason that is still undissolved except for dimension errors. In addition, although C4, C5 and C6 in Figure 7 right have same window size each with Figure 7 left, it is equivalent to the half dimension of Figure 7 left by the effect of the electric wall. Though the mode matching method and the measurement value are in relatively good agreement, it did not lead to an exact match such as the case of the inductive window. There is still room for discussion for the capacitive cause.

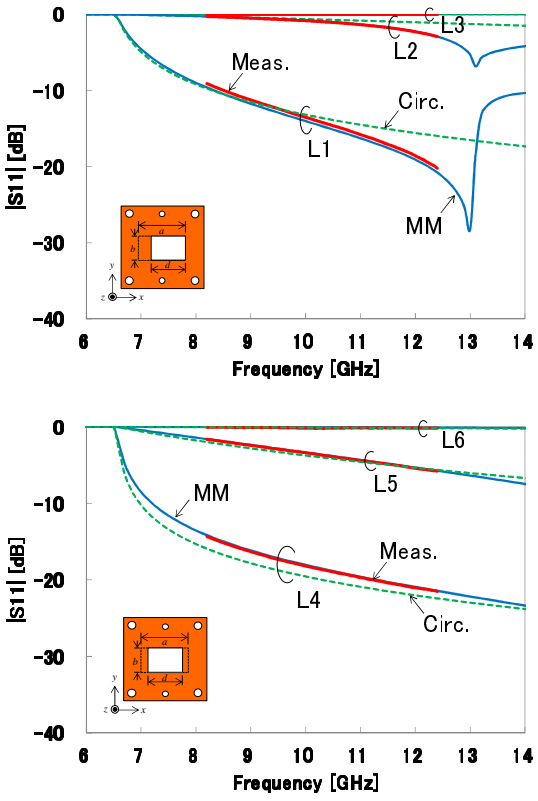

Fig. 6. Measurement result.

Inductive window L1, L2, L3 (left). Inductive window L4, L5, L6 (right).

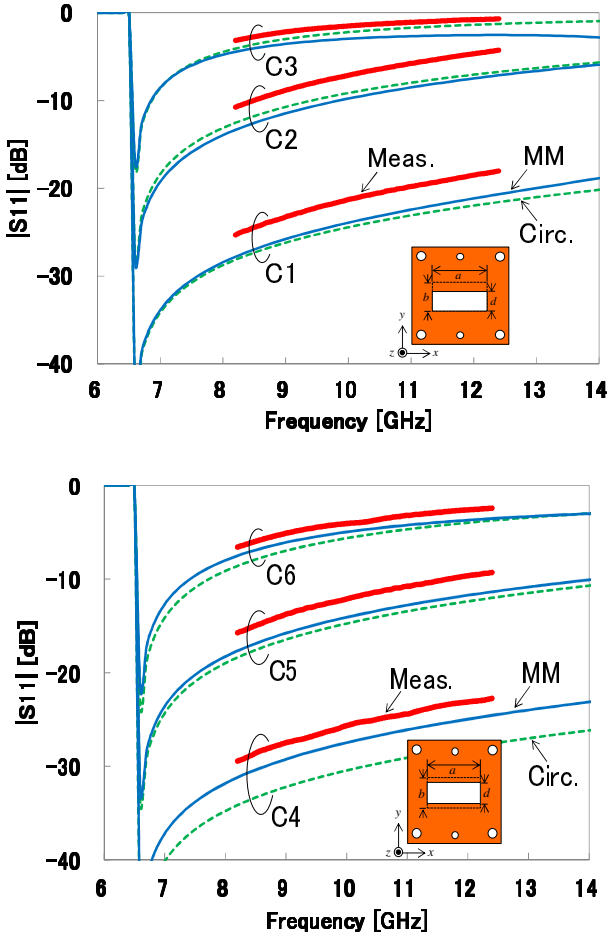

Fig. 7. Measurement result. Capacitive window C1, C2, C3 (Left). Capacitive window C4, C5, C6 (Right).

5. CONCLUSIONS

In the part of the educational program for training high-frequency engineers, the waveguide L and C samples which have reduced manufacturing error were fabricated as new waveguide loads to be used in the microwave student experiment and its characteristics were measured and calculated. The equivalent circuit calculation and the mode matching method were considered as theoretical values. Then these two calculation methods were compared with the measured values.

As a result, the frequency characteristics of each sample were confirmed to be a relatively good agreement.

Although inductive window was completely matched with the exact solution, it was found that the capacitive window has a difference that is not able be tolerated as an experimental standard. Since it is considered that there is a cause that is not still clear except for dimension errors and will be discussed in detail in the future.

ACKNOWLEDGEMENT

This research was subsidized by the scientific research fund 26750073, "Development of RF design engineer training program," young scientists (B).

REFERENCES

[1] Takeda, Y. A Radio Wave and Frequency Textbook, Impress, 2005, 54-63.

[2] Shiga S. The Request from a Microwave Device Company to lnstitutions of a Higher Education, 2008, Proceedings of Institute of Electronics, Information, and Communication Engineers Japan, 2008, electronics 1, S29-S30.

[3] Kawasaki S. Education in a University for Microwave Solid-State Circuits : Class and Laboratory for the Circuit Design Using a Simulator, Proceedings of Institute of Electronics, Information, and Communication Engineers Japan, 2002, 344.

[4] Vindevoghel, M.; Hochedez, M.; Legier, J. F.et al. Multimedia self training product for microwave learning, Conf. Proc. EuMC, 1990, 20 (1), 729-733.

[5] McIntosh, R. E.; Monaghan, S. R.; Temple S. J. Microwave educational program: An industry university alliance. IEEE Trans. Educ. 1983, 26 (4), 143-151.

[6] Fernandes, H. C. C.; Giarola, A. J; Rogers, D. A. PACMO: A comprehensive CAD package for microwave devices, IEEE Trans. Educ. 1983, 26 (4), 162-164.

[7] Pozar, D. M. A Modern Course in Microwave Engineering,'' IEEE Trans. Educ. 1990, 33 (1), 129-134.

[8] Menzel, W. Microwave Education Supported by Animations of Wave Propagation Effects, IEEE Trans. MTT. 2003, 51 (4), 1312-1317.

[9] Kazuhiko H. Advanced Seminar using Microwave CAD - A New Trend for Seminars in Universities for Professional. The University of Electro-Communications Bulletin. 2004, 16 (2), 169-177.

[10] I-Laboratory High Frequency Circuit Design Technology in GHz Era, http://www1.sphere.ne.jp/i-lab/.

[11] Keysight Technologies, High-frequency Measurement Engineering on Microwave Technology, Special lecture for doctoral course in graduate school of Tohoku University. http://www.keysight.com/.

[12] Y. Kusama, O. Hashimoto, A Study on Development of Experimental Student Program for RF Engineer Training - High-Frequency Impedance Measurement with Waveguide Standing Wave Method, Institute of Electronics, Information, and Communication Engineers Japan, Technical report. 2014, ET2014-35, 35-40.

[13] Kusama Y.S.; Masayuki, O. H. Fabrication and Characteristics Measurement of a Waveguide Reactance Element - For experimental graduate student program in microwave engineering, Japan Society for Engineering Education 62nd annual convention. 2014, 3F07, .538-539.

[14] Konishi, Y. High Frequency and Microwave Circuit - Basis and design, Keirabo publication, 2003, .277.

[15] Kawasaki, S.; Nakatani, A. CAD Deign I of Microwave Planar Circuit - Passive circuit, Realize Inc., 1996, 77-84.

[16] Pozar, D. M. Microwave Engineering - 4th edition, Wiley, 2011, 203-209.

[17] Hongo, K. Basis of the electromagnetic field and the calculation method, Shinzansha scitech, 1993, 84-85.

[18] Uher; BornemannL; Rosenberg. Waveguide Components for Antenna Feed Systems: Theory and CAD, Artech House, 1993, .9-27.

[19] Kyo, Z. CAD Programs for Microwave Circuit Engineers and Researchers, Mimatsu data, 1998, 69-124.

[20] Chu T. S. Generalized Scattering Matrix Method for Analysis of Cascaded and Offset Microstrip Step Discontinuities. IEEE Trans. MTT, 1986, 34, 280-284.